JACS
JOURNAL OF THE AMERICAN CHEMICAL SOCIETY

COMMUNICATION

pubs.acs.org/JACS

# Iron(II) PARACEST MRI Contrast Agents

Sarina J. Dorazio,[†,‡] Pavel B. Tsitovich,[†,‡] Kevin E. Siters,[†] Joseph A. Spernyak,[§] and Janet R. Morrow*[,†]

[†]Department of Chemistry, University at Buffalo, State University of New York, Amherst, New York 14260, United States
[§]Department of Cell Stress Biology, Roswell Park Cancer Institute, Buffalo, New York 14263, United States

Supporting Information

**ABSTRACT:** The first examples of Fe(II) PARACEST magnetic resonance contrast agents are reported (PARACEST = paramagnetic chemical exchange saturation transfer). The iron(II) complexes contain a macrocyclic ligand, either 1,4,7-tris(carbamoylmethyl)-1,4,7-triazacyclononane (**L1**) or 1,4,7-tris[(5-amino-6-methyl-2-pyridyl)methyl]-1,4,7-triazacyclononane (**L2**). The macrocycles bind Fe(II) in aqueous solution with formation constants of log $K$ = 13.5 and 19.2, respectively, and maintain the Fe(II) state in the presence of air. These complexes each contain six exchangeable protons for CEST which are amide protons in $[Fe(\mathbf{L1})]^{2+}$ or amino protons in $[Fe(\mathbf{L2})]^{2+}$. The CEST peak for the $[Fe(\mathbf{L1})]^{2+}$ amide protons is at 69 ppm downfield of the bulk water resonance whereas the CEST peak for the $[Fe(\mathbf{L2})]^{2+}$ amine protons is at 6 ppm downfield of bulk water. CEST imaging using a MRI scanner shows that the CEST effect can be observed in solutions containing low millimolar concentrations of complex at neutral pH, 100 mM NaCl, 20 mM buffer at 25 °C or 37 °C.

An intriguing approach in magnetic resonance imaging (MRI) is the development of contrast agents that utilize endogenous transition metal ions. Such contrast agents would provide a safer alternative to lanthanide(III) (Ln(III)) contrast agents for patients with compromised kidney function.[1] In addition, the distinct coordination chemistry of transition metal ions facilitates the design of new ligands and approaches for responsive or smart contrast agents that cannot be used with Ln(III) ions.[2] Here we present the first examples of Fe(II) MRI contrast agents that function through chemical exchange saturation transfer (PARACEST or CEST) MRI. PARACEST agents contain groups with exchangeable protons such as NH or OH functional groups. Application of a radiofrequency pulse at the frequency of the exchangeable proton partially saturates the magnetization of the proton and, through exchange, decreases the intensity of the bulk water signal.[3,4] The paramagnetic metal ion serves to shift the exchangeable proton resonances far from the bulk water resonant frequency, leading to a reduction in interference from magnetization transfer effects.[5]

High spin octahedral Fe(II) complexes are ideal for PARACEST because the paramagnetic center induces a large ligand proton shift but has a relatively low relaxivity.[6] PARACEST agents require low relaxivity because shortened $T_2$ times lead to broad line widths, reducing saturation efficiency and requiring higher transmitter power for saturation of the exchangeable pool of protons. We show here that Fe(II) PARACEST agents have comparable or larger induced proton chemical shifts (>200 ppm) than many Ln(III) complexes and show CEST images at concentrations similar to those of Ln(III) PARACEST agents.[3]

Fe(II) PARACEST agents were developed by preparing ligands that stabilize the Fe(II) oxidation state, contain multiple exchangeable protons to enhance the CEST effect and form six coordinate complexes to protect the Fe(II) from binding additional ligands that might complicate the CEST signal. Our hexadentate ligands contained the macrocycle, 1,4,7-triazacyclononane, with three pendant groups (Chart 1). Pyridine pendant groups stabilize Fe(II) relative to Fe(III), leading to reduction potentials as high as 1.0 V vs NHE for $[Fe(\mathbf{L3})]^{2+}$ and giving air stable complexes.[7,8] Amide pendant groups are moderately stabilizing of the Fe(II) oxidation state.[9] For CEST agents, exchangeable protons close to the Fe(II) center as well as more remotely located protons appended to a ligand pi-system were studied in order to capitalize on both the dipolar and contact shift contributions of paramagnetic Fe(II).[6] Amide groups such as those in **L1** contain exchangeable NH protons that are located three bonds away from the metal ion center and have been successfully used for Ln(III) PARACEST agents.[10] In contrast, the aminopyridine pendant groups in **L2** have exchangeable protons attached to a pi-system that are four bonds removed from the Fe(II) and have not been previously used for PARACEST agents.

$[Fe(\mathbf{L1})]^{2+}$ and $[Fe(\mathbf{L2})]^{2+}$ were prepared in aqueous solution by addition of the ligands to $Fe(CF_3SO_3)_2$. The formation constants of $[Fe(\mathbf{L1})]^{2+}$ and the related complex $[Fe(\mathbf{L3})]^{2+}$ as determined by pH−potentiometric titrations were log $K$ = 13.5 and 19.2, respectively, in 100 mM NaCl, demonstrating strong binding of the macrocycles to Fe(II) (Tables S2 and S3 and Figures S1 and S2 in the Supporting Information). Speciation diagrams show that $[Fe(\mathbf{L2})]^{2+}$ and $[Fe(\mathbf{L1})]^{2+}$ are the predominant species at neutral pH.

Complexes of **L1** and **L2** are predominantly high spin (HS) Fe(II) in aqueous solution. Effective magnetic moments are characteristic of HS Fe(II) at 5.1 $\mu_B$ and 5.8 $\mu_B$ for $[Fe(\mathbf{L1})]^{2+}$ and $[Fe(\mathbf{L2})]^{2+}$, respectively, at pH 7.2, 25 °C (eq S1 in the Supporting Information).[11] Furthermore, the relatively narrow line widths of the $^1$H NMR resonances of the complexes are characteristic of HS Fe(II) and not HS Fe(III). Importantly, it is only the HS Fe(II) complexes that give rise to the highly shifted narrow proton resonances used for PARACEST experiments. The $^1$H NMR spectra of the complexes are shown in Figures S3 and S4 in the Supporting Information. There are nine nonexchangeable proton resonances for $[Fe(\mathbf{L2})]^{2+}$ consistent with a pseudo-octahedral geometry as observed previously[7] for

**Received:** May 10, 2011
**Published:** August 12, 2011

**Chart 1. Fe(II) Complexes for PARACEST**

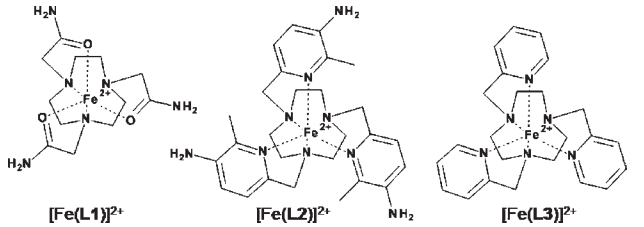


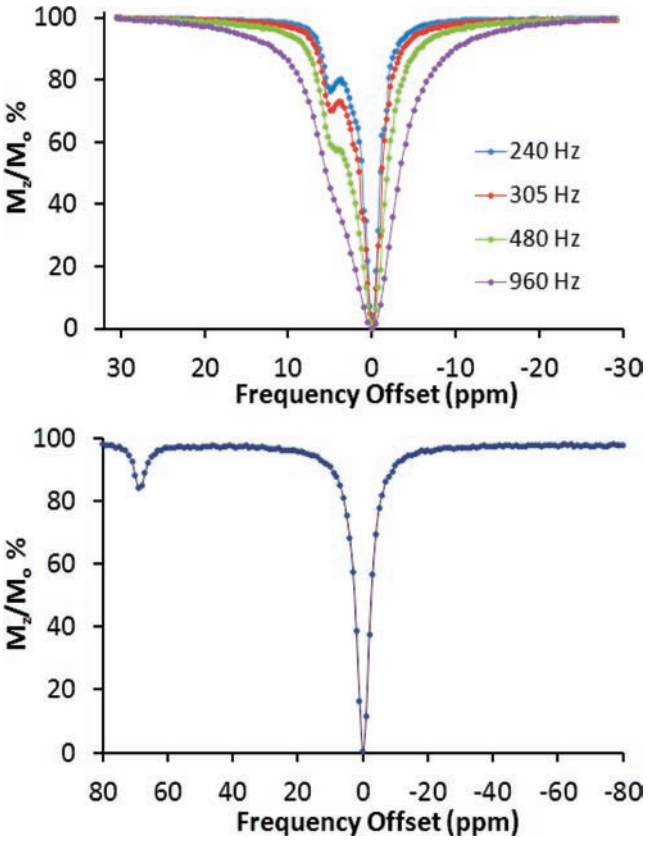


**Figure 1.** CEST spectra recorded at 400 MHz of (top) 4 mM $[Fe(L2)]^{2+}$, pH 7.0 at 25 °C with $B_1$ as shown and 4 s presaturation pulse, and (bottom) 8 mM $[Fe(L1)]^{2+}$ 20 mM HEPES pH 6.8, 100 mM NaCl, 37 °C, with $B_1$ = 960 Hz, 4 s.

$[Fe(\mathbf{L3})]^{2+}$ and with a rigid structure that leads to three sets of four chemically inequivalent proton resonances in the macrocycle backbone. The three broad proton resonances for non-exchangeable protons in the $^1$H NMR spectrum of $[Fe(\mathbf{L1})]^{2+}$ show that there is a dynamic process on the NMR time scale that averages the protons in the macrocyclic backbone, giving rise to two broad peaks instead of four as in $[Fe(\mathbf{L2})]^{2+}$ and one broad peak instead of two for the methylene protons of the pendant group. The exchangeable protons were identified by comparison of the $^1$H NMR spectra of the complexes in $D_2O$ and $CD_3CN$. For $[Fe(\mathbf{L1})]^{2+}$, one of the amide protons is highly shifted downfield, appearing at 77 ppm, and the other is upfield appearing at 4 ppm in $CD_3CN$. This large separation between proton resonances of the amides is similar to that reported previously for Fe(II) complexes,[12] but unlike that typically

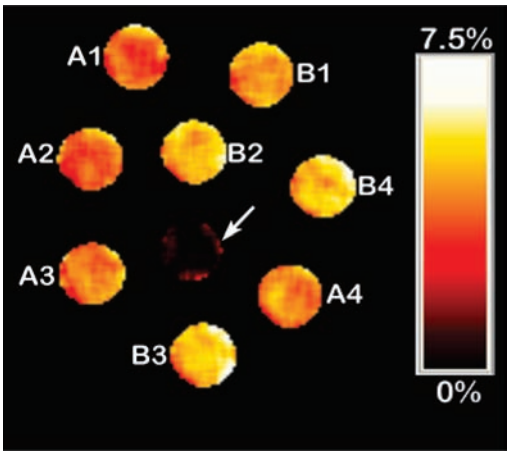


**Figure 2.** CEST images of phantoms on a MRI 4.7 T scanner. Arrow: buffer only. Other samples contain $[Fe(L1)]^{3+}$: A1 (pH 6.8, 2 mM), A2, (pH 6.8, 3 mM), A3 (pH 6.7 6 mM), A4 (pH 6.8, 8 mM), B1 (pH 7.2, 2 mM) B2 (pH 7.2, 3 mM), B3 (pH 7.1, 6 mM), B4 (pH 7.1, 8 mM) at 37 °C, with 20 mM Hepes and 100 mM NaCl. Scale represents loss of signal due to CEST saturation pulse.

observed for Ln(III) PARACEST agents that contain amide groups.[10] The amine protons of $[Fe(\mathbf{L2})]^{2+}$ are less highly shifted and are observed at 11 ppm in $CD_3CN$. No other exchangeable protons are expected given that the hexadentate ligands coordinatively saturate the Fe(II). The $^1$H NMR spectrum of $[Fe(\mathbf{L2})]^{2+}$ and the $\mu_{eff}$ of $[Fe(\mathbf{L1})]^{2+}$ did not change over several days, consistent with the persistence of the Fe(II) oxidation state in neutral aqueous solution.

CEST spectra, plotted as the percent reduction of the water proton resonance as a function of the presaturation frequency, are shown in Figure 1 for $[Fe(\mathbf{L1})]^{2+}$ and $[Fe(\mathbf{L2})]^{2+}$ at near neutral pH. $[Fe(\mathbf{L1})]^{2+}$ gives a CEST peak at 69 ppm versus bulk water, arising from the amide protons. $[Fe(\mathbf{L2})]^{2+}$ gives a CEST shoulder at 6 ppm versus bulk water, attributed to exchange of the amine protons. CEST spectra as a function of presaturation pulse power are given for $[Fe(\mathbf{L2})]^{2+}$ to better show definition of the shoulder in the CEST spectrum. For $[Fe(\mathbf{L1})]^{2+}$, the CEST peak is substantially larger at 37 °C than at 25 °C, while $[Fe(\mathbf{L2})]^{2+}$ shows a very modest increase in CEST effect with temperature (Figure S5 in the Supporting Information). The marked increase in the CEST peak for $[Fe(\mathbf{L1})]^{2+}$ with temperature is attributed to a near doubling in the rate constant for exchange of the amide proton (220 $s^{-1}$ at 25 °C).

To validate the observed CEST spectra of the Fe(II) complexes, CEST imaging was done on a 4.7 T scanner using a phantom array containing solutions of $[Fe(\mathbf{L1})]^{2+}$ at different concentrations as shown in Figure 2. A pair of gradient echo images were acquired with a presaturation pulse either on resonance (69 ppm) or off resonance (−69 ppm) of the exchangeable protons. The ratio between these two images is subtracted from 100% to generate a CEST image. The wells labeled A1−A4 and B1−B4 contained solutions of $[Fe(\mathbf{L1})]^{2+}$ with NaCl and buffer at acidic (A) or basic (B) pH. The phantoms show that CEST increases with concentration of the Fe(II) complex (Figure S6 in the Supporting Information) and improves at basic pH due to an increase in proton exchange rate constant. Similarly CEST imaging of $[Fe(\mathbf{L2})]^{2+}$ shows increasing CEST over the concentration range 1−3 mM (Figure S6 in the Supporting Information). $T_1$ and $T_2$ relaxivities for both complexes

are relatively low at 0.21 and 0.28 $mM^{-1}s^{-1}$ for $[(Fe(\mathbf{L1})]^{2+}$ and 0.021 and 0.14 $mM^{-1}s^{-1}$ for $[(Fe(\mathbf{L2})]^{2+}$ (Table S4 in the Supporting Information). Note that the $T_1$ values for the Fe(II) complexes here are comparable to those of Eu(III) complexes.[13]

In summary, we report PARACEST agents that, for the first time, contain the biologically important transition metal ion, Fe(II). The complexes are stable as high spin Fe(II) under physiologically relevant conditions and contain multiple protons for exchange with bulk water. The dipolar and contact shift contributions of paramagnetic Fe(II) complexes make it feasible to use donor groups with exchangeable protons such as the NH of amides as well as more remotely located groups connected through a pyridine pi-system. This opens up entire new classes of ligands for PARACEST agents with different possible donor groups. Such iron containing MRI contrast agents may be developed as alternatives to lanthanide(III) analogues for patients with impaired kidney function and susceptibility to nephrogenic systemic fibrosis.[1]

## ■ ASSOCIATED CONTENT

**Supporting Information.** Materials/methods, synthesis, NMR spectra, potentiometric titrations. This material is available free of charge via the Internet at http://pubs.acs.org.

## ■ AUTHOR INFORMATION

### Corresponding Author
jmorrow@buffalo.edu

### Author Contributions
‡Authors contributed equally to manuscript.

## ■ ACKNOWLEDGMENT

We gratefully acknowledge the National Science Foundation (CHE-0911375) and the National Institutes of Health (EB-04609) for support of this work.

## ■ REFERENCES

(1) Rydahl, C.; Thomsen, H. S.; Marckmann, P. *Invest. Radiol.* **2008**, *43*, 141–144.
(2) Gispert, J. R. *Coordination Chemistry*; Wiley VCH Verlag GmbH & Co KGaA: Weinheim, 2008.
(3) Viswanathan, S.; Kovacs, Z.; Green, K. N.; Ratnakar, S. J.; Sherry, A. D. *Chem. Rev.* **2010**, *110*, 2960–3018.
(4) Sherry, A. D.; Woods, M. *Mol. Cell. MR Imaging* **2007**, 101–122.
(5) Ali, M. M.; Liu, G.; Shah, T.; Flask, C. A.; Pagel, M. D. *Acc. Chem. Res.* **2009**, *42*, 915–924.
(6) Bertini, I.; Luchinat, C.; Parigi, G.; Pierattelli, R. *ChemBioChem* **2005**, *6*, 1536–1549.
(7) Wieghardt, K.; Schöffmann, E.; Nuber, B.; Weiss, J. *Inorg. Chem.* **1986**, *25*, 4877–4883.
(8) Christiansen, L.; Hendrickson, D. N.; Toftlund, H.; Wilson, S. R.; Xie, C.-L. *Inorg. Chem.* **1986**, *25*, 2813–2818.
(9) Mandal, S. K.; Que, L., Jr. *Inorg. Chem.* **1997**, *36*, 5424–5425.
(10) Zhang, S.; Michaudet, L.; Burgess, S.; Sherry, A. D. *Angew. Chem., Int. Ed.* **2002**, *41*, 1919–1921.
(11) Stavila, V.; Allali, M.; Canaple, L.; Stortz, Y.; Franc, C.; Maurin, P.; Beuf, O.; Dufay, O.; Samarut, J.; Janier, M.; Hasserodt, J. *New J. Chem.* **2008**, *32*, 428–435.
(12) Ming, L.-J.; Lauffer, R. B.; Que, L., Jr. *Inorg. Chem.* **1990**, *29*, 3060–3064.
(13) Huang, C.-H.; Morrow, J. R. *Inorg. Chem.* **2009**, *48*, 7237–7243.